Supporting Information

Unconventionally Crafting Defect-Rich NiO Nanoparticles within Ultrathin Metal-organic Frameworks Nanosheets to Enable High-Output Oxygen Evolution

*Qi Hu, Xiaowan Huang, Ziyu Wang, Guomin Li, Zhen Han, Hengpan Yang, Xiangzhong Ren, Qianling Zhang, Jianhong Liu and Chuanxin He**

College of Chemistry and Environmental Engineering, Shenzhen University, Shenzhen, Guangdong, 518060, People's Republic of China.

*To whom correspondence should be addressed. Email: hecx@szu.edu.cn (C. He)

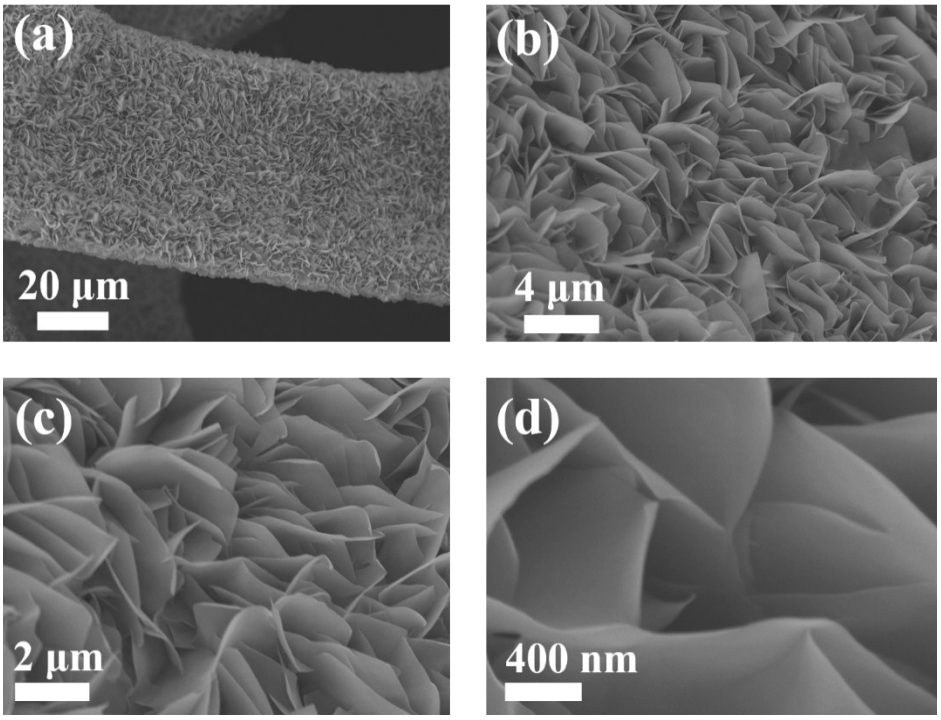

Figure S1 SEM images of 2D Ni-MOF precursors, which were prepared via a microwave-assisted hydrothermal method.

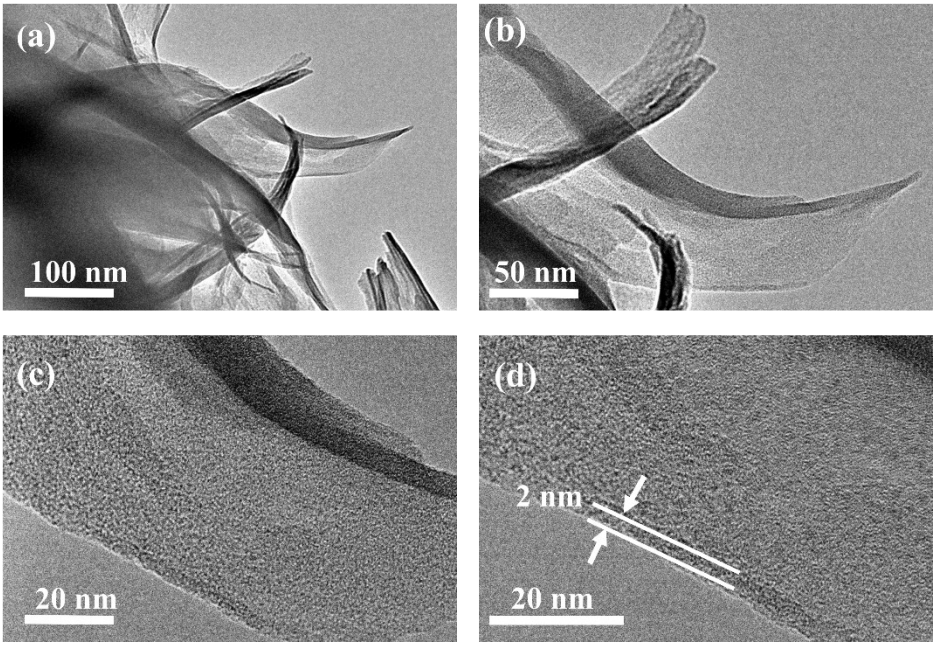

Figure S2 (a, b) TEM, and (c, d) HRTEM images of 2D Ni-MOF precursors.

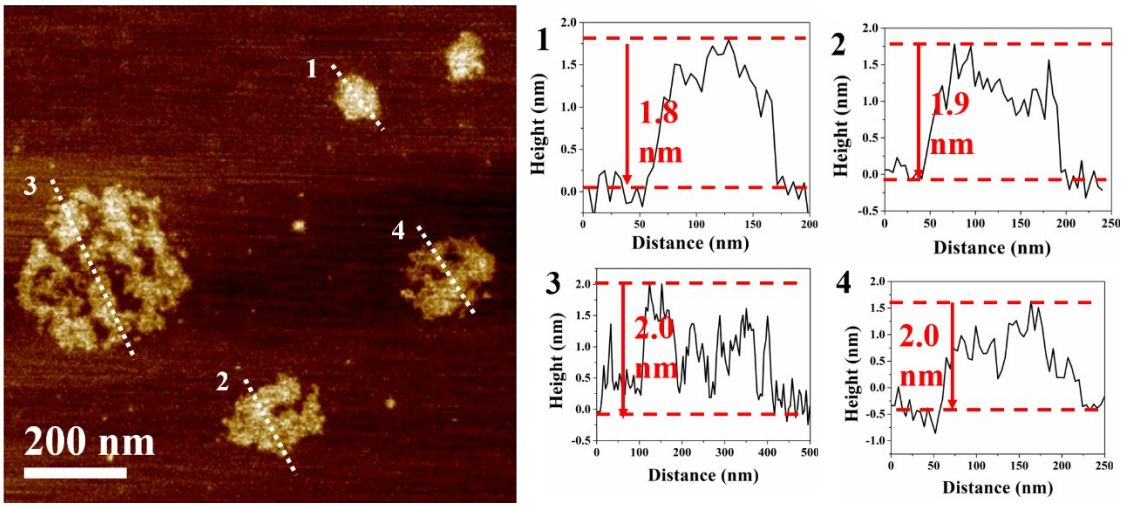

Figure S3 AFM images of 2D Ni-MOF precursors, and the thickness of nanosheets on the 2D Ni-MOF

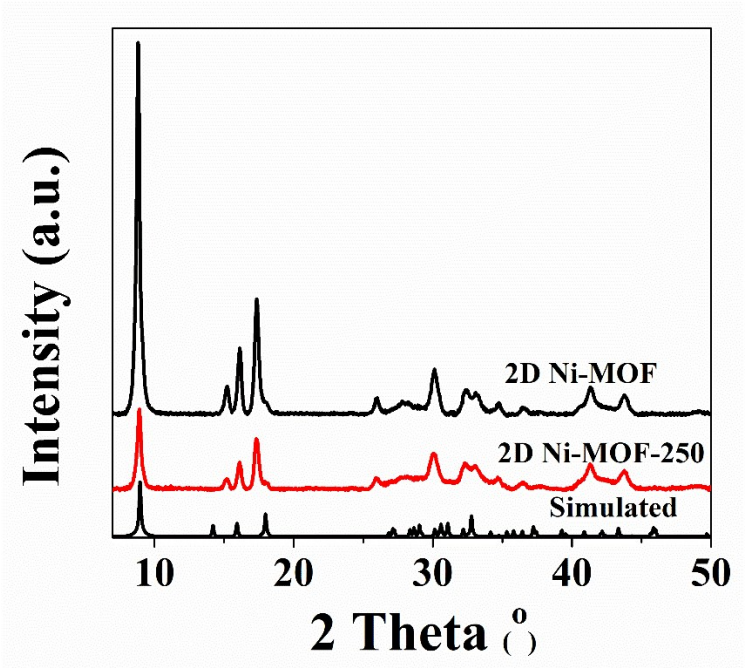

Figure S4 XRD patterns of 2D Ni-MOF, and 2D Ni-MOF-250. The 2D Ni-MOF-250 was prepared through the calcination of 2D Ni-MOF precursors at 250 °C in air.

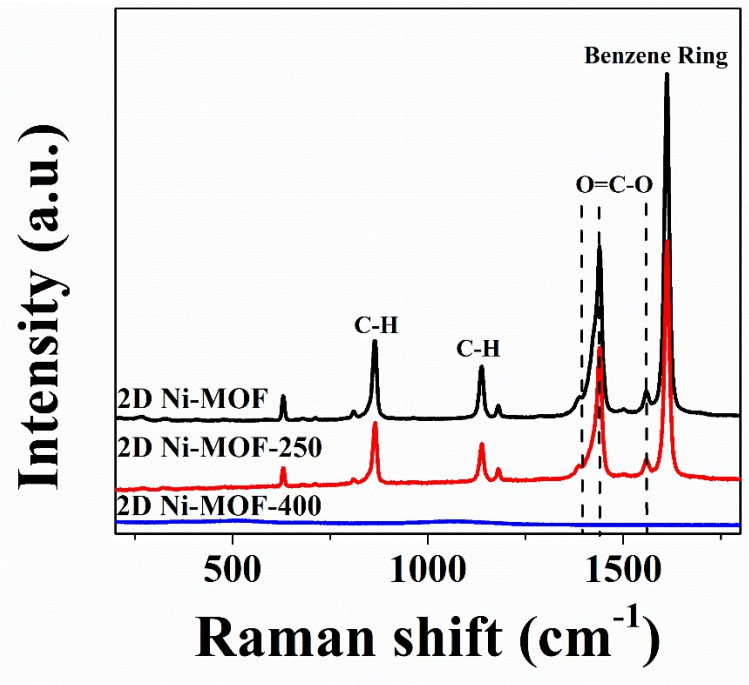

Figure S5 Raman spectra of 2D Ni-MOF, 2D Ni-MOF-250, 2D Ni-MOF-400. The 250 and 400 represent the calcination temperature.

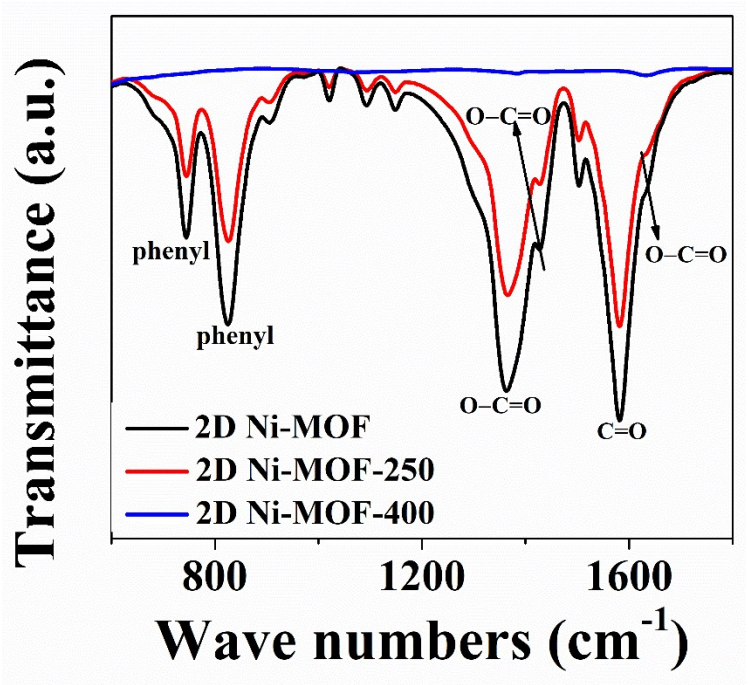

Figure S6 FT-IR spectra of 2D Ni-MOF, 2D Ni-MOF-250, and 2D Ni-MOF-400.

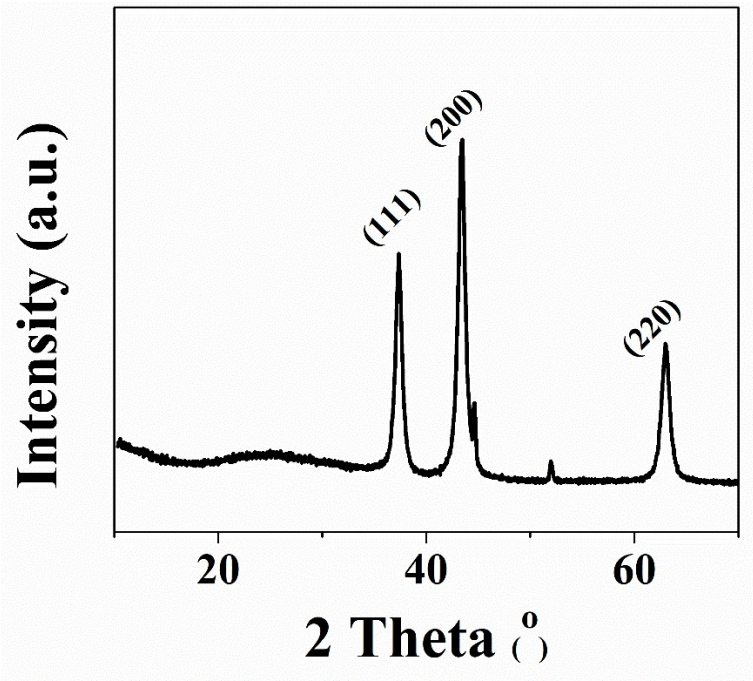

Figure S7 XRD patterns of 2D Ni-MOF-400.

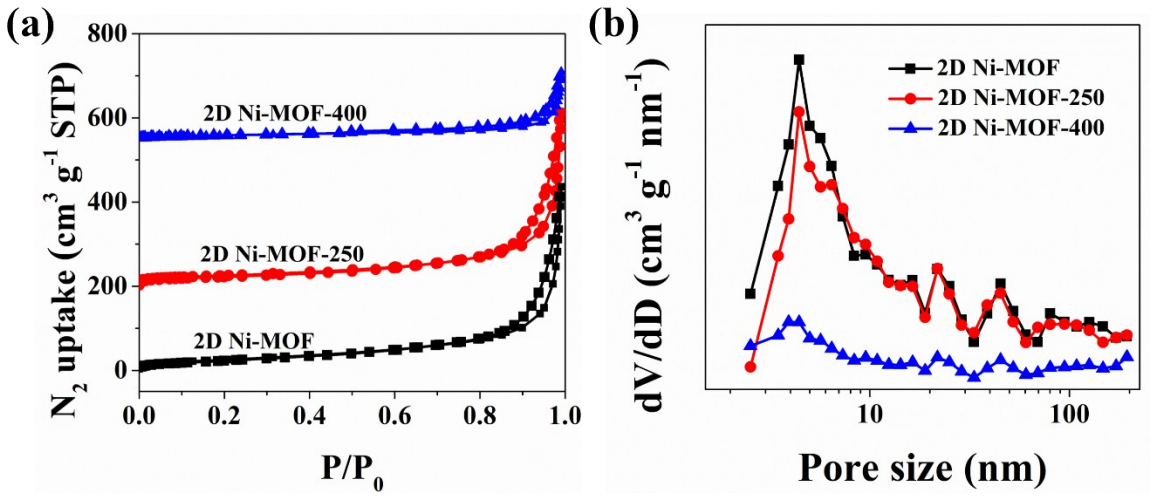

Figure S8 (a) N_2 adsorption−desorption isotherm and (b) corresponding pore distribution of 2D Ni-MOF, 2D Ni-MOF-250, and 2D Ni-MOF-400.

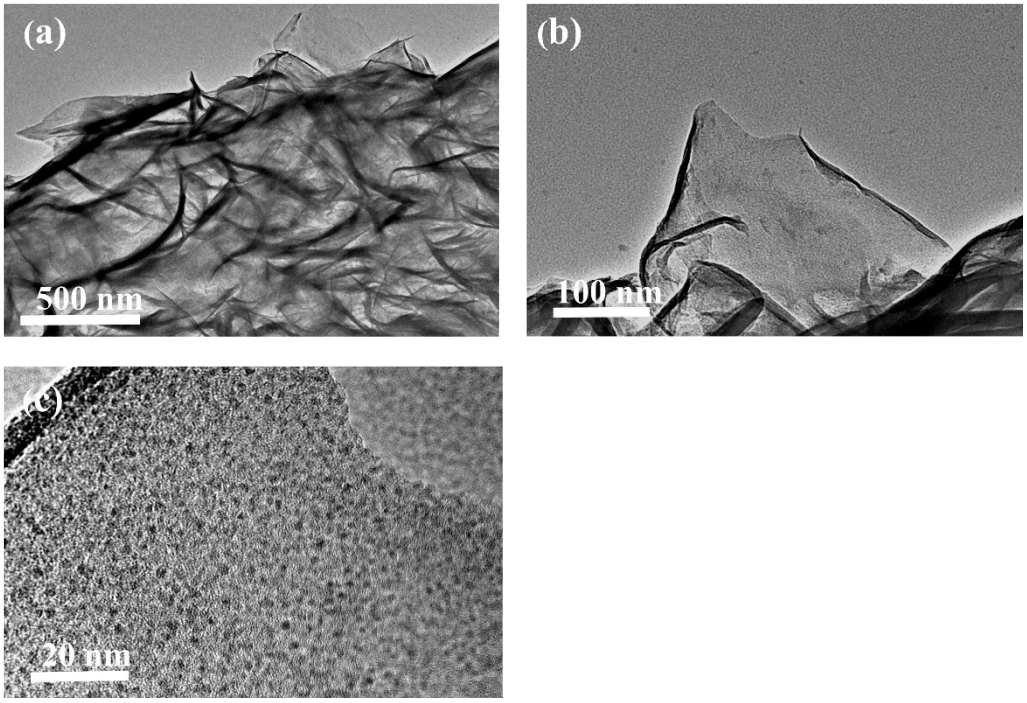

Figure S9 TEM imges of 2D Ni-MOF-250-1. The 2D Ni-MOF-250-1 was synthesized through the similar process of 2D Ni-MOF-250 but the calcination time shortened to 1 h.

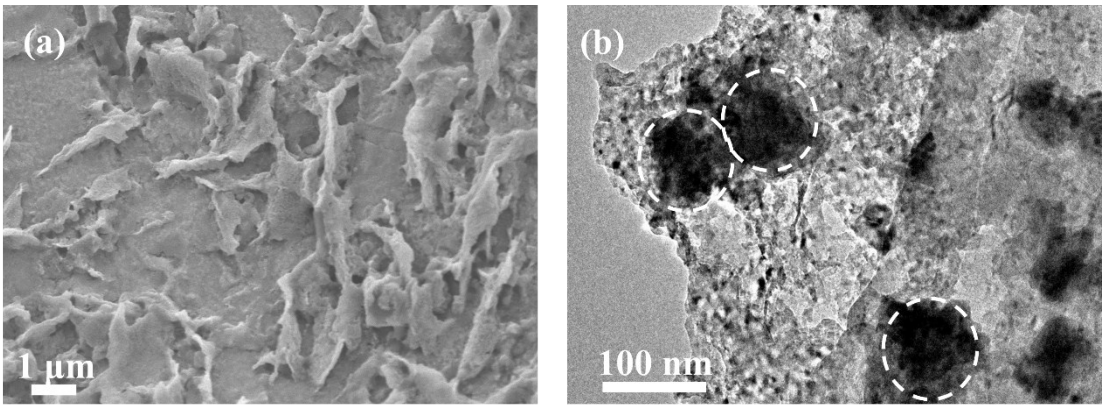

Figure S10 SEM and TEM images of 2D Ni-MOF-400.

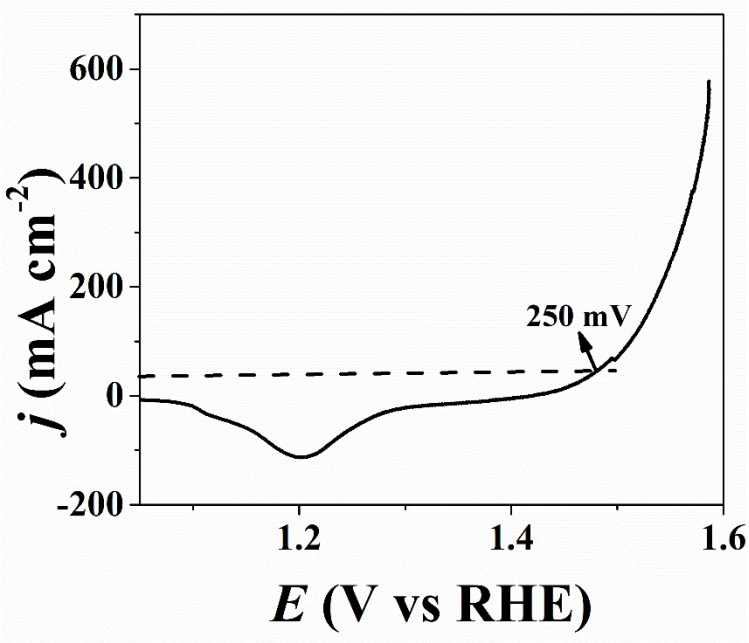

Figure S11 LSV of 2D Ni-MOF-250, which obtained by sweeping from the high to low potential.

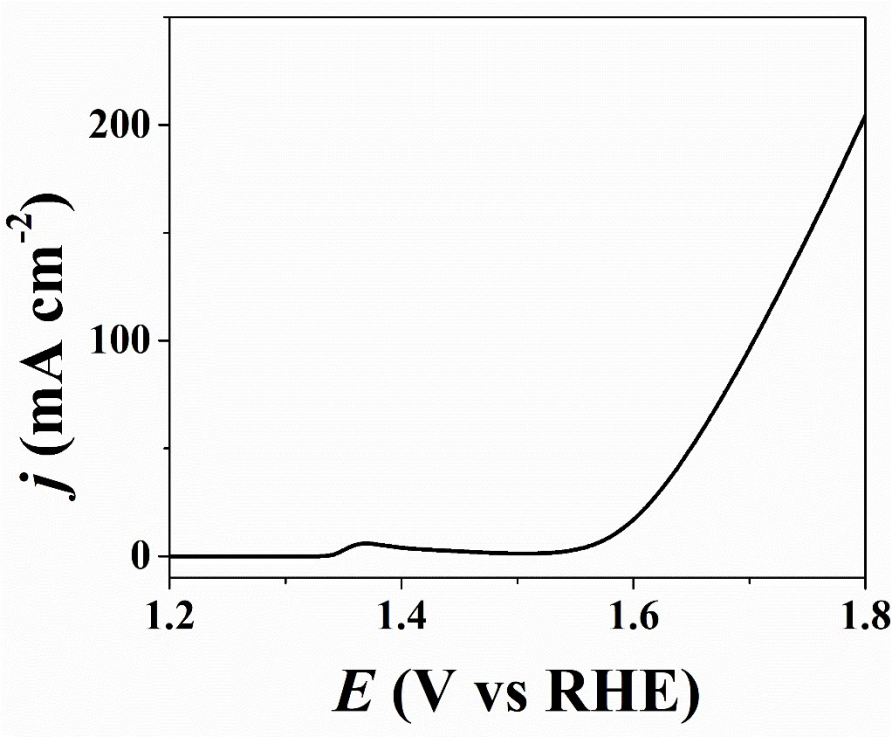

Figure S12 LSV of pure Ni foams for OER in 1 M KOH.

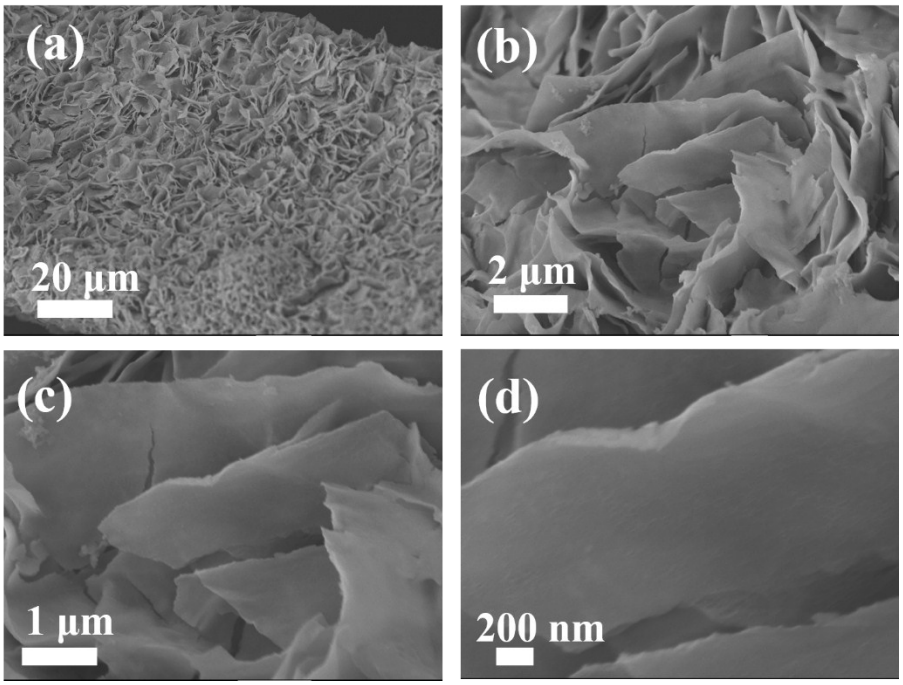

Figure S13 SEM images of 2D Ni-MOF-250 after the stability test of 20 h.

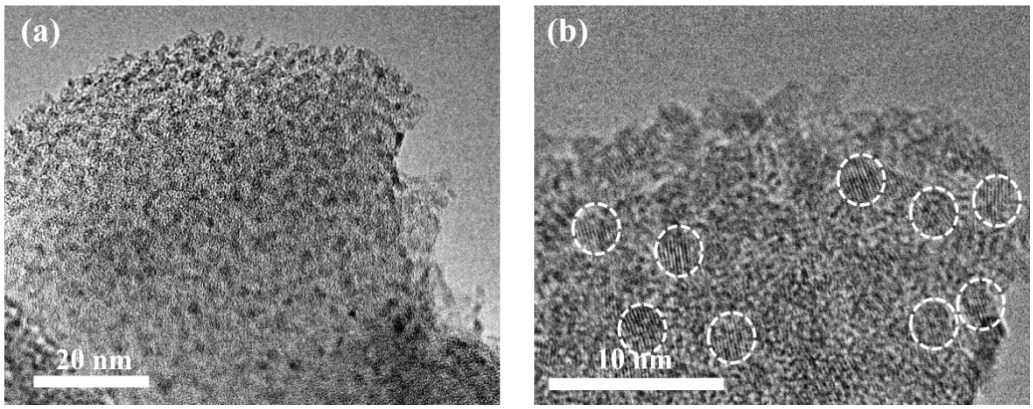

Figure S14 (a) TEM and (b) HRTEM images of 2D Ni-MOF-250 after the stability of 20 h.

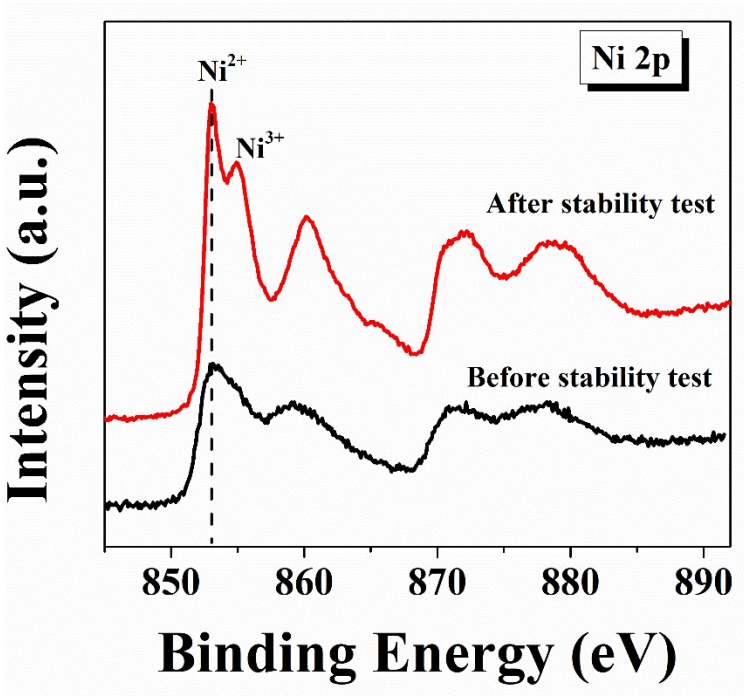

Figure S15 Ni 2p XPS spectra of 2D Ni-MOF-250 before and after the stability of 20 h.

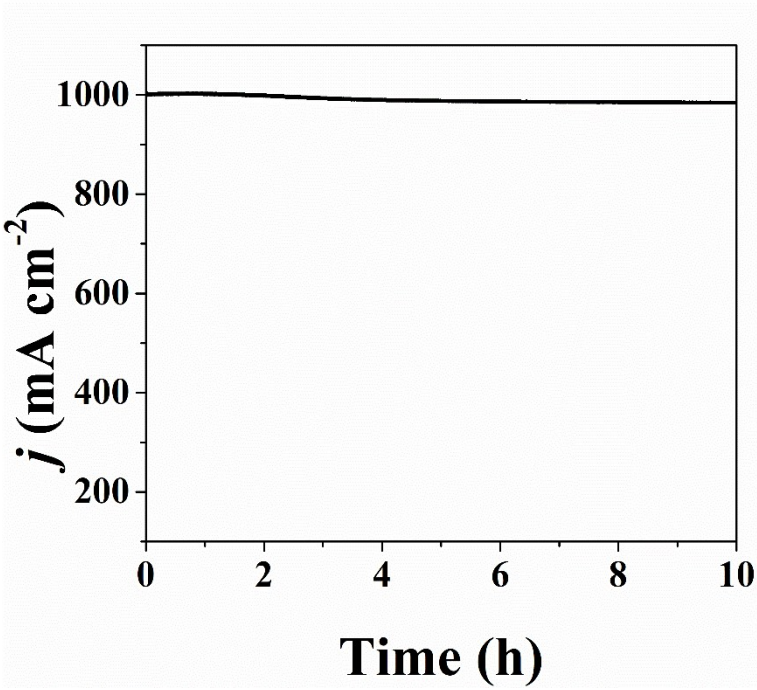

Figure S16 Stability test of 2D Ni-MOF-250 at the current density of 1000 mA cm^{-2}.

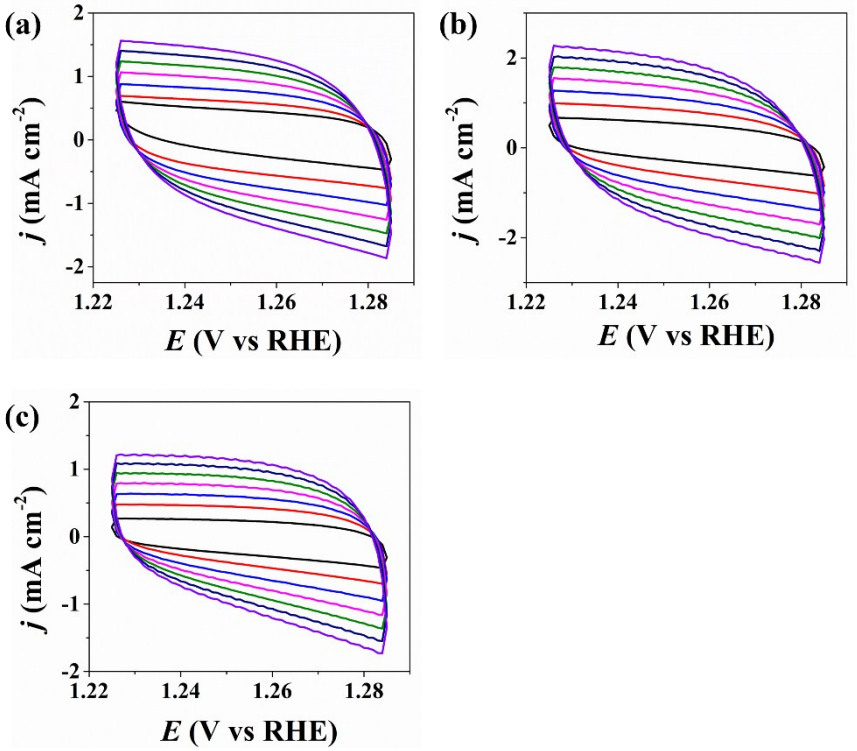

Figure S17 CV curves for (a) 2D Ni-MOF, (b) 2D Ni-MOF-250, and (c) 2D Ni-MOF-400 at different scan rates (i.e., 0.04, 0.06, 0.08, 0.10, 0.12, 0.14 and 0.16 V s^{-1}).

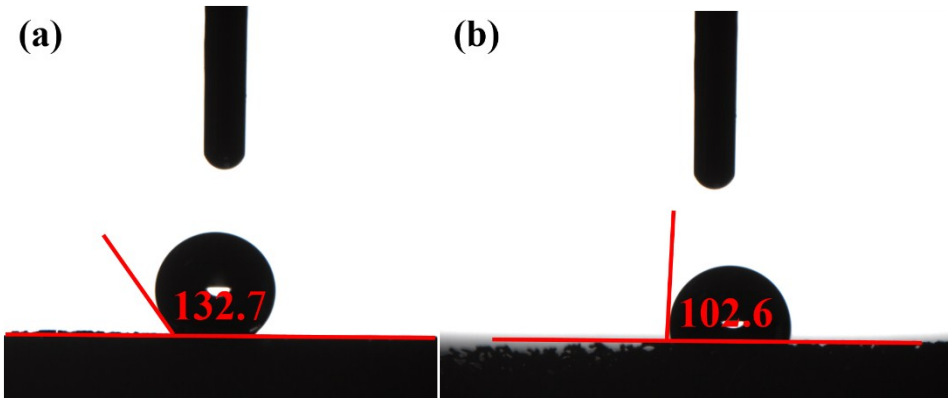

Figure S18 Water contact angles of a drop water on (a) pure Ni foams, and (b) 2D Ni-MOF-250

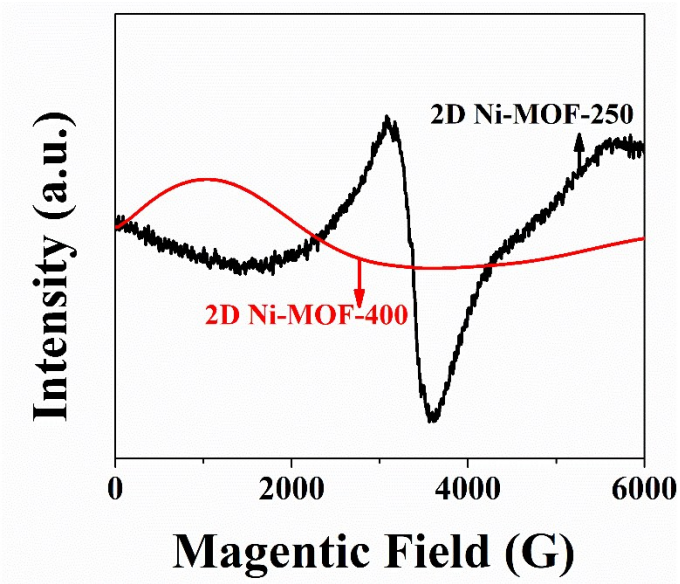

Figure S19 ESR spectra of 2D Ni-MOF-250, and 2D Ni-MOF-400.

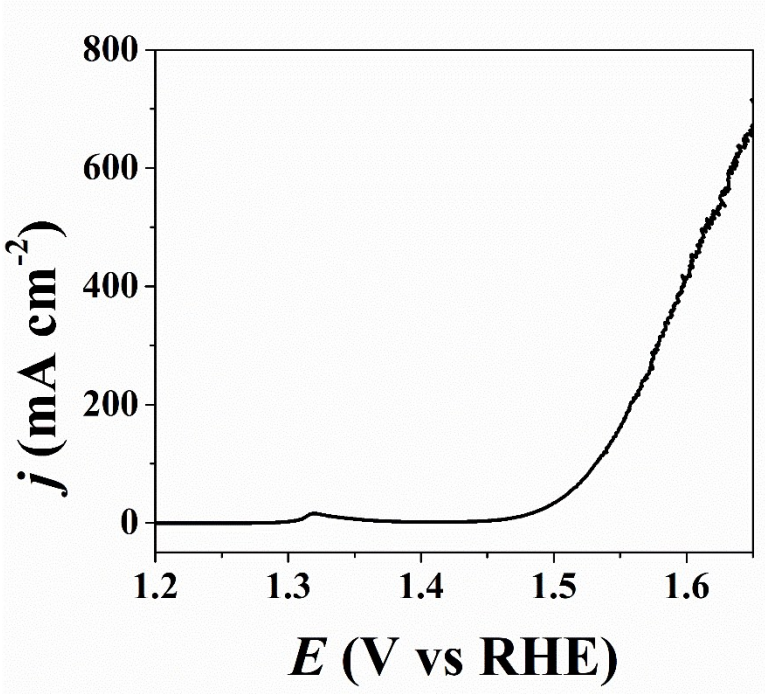

Figure S20 LSV of 2D Ni-MOF-250-1 for OER in 1 M KOH.

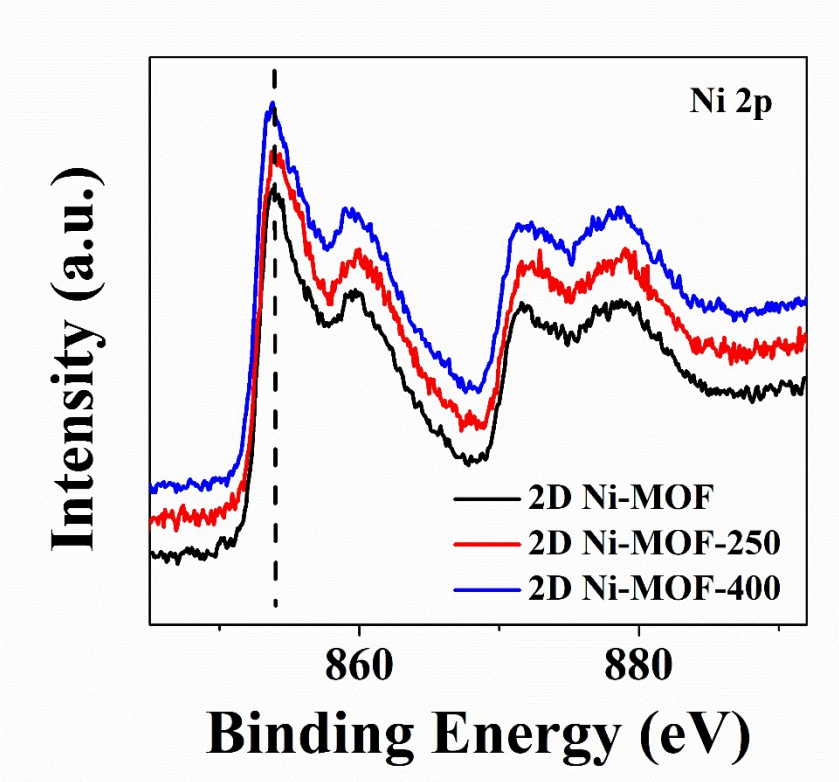

Figure S21 XPS spectra of Ni 2p for 2D Ni-MOF, 2D Ni-MOF-250, and 2D Ni-MOF-400.